methods

Characterization and direct quantitation of cerebroside molecular species from lipid extracts by shotgun lipidomics

Xianlin Han[1] and Hua Cheng

Division of Bioorganic Chemistry and Molecular Pharmacology, Department of Medicine, Washington University School of Medicine, St. Louis, MO 63110

Abstract **By using shotgun lipidomics based on the separation of lipid classes in the electrospray ion source (intrasource separation) and two-dimensional (2D) MS techniques (Han, X., and R. W. Gross. 2004. Shotgun lipidomics: electrospray ionization mass spectrometric analysis and quantitation of the cellular lipidomes directly from crude extracts of biological samples. *Mass Spectrom. Rev.* First published on June 18, 2004; doi: 10.1002/mas.20023, In press), individual molecular species of most major and many minor lipid classes can be quantitated directly from biological lipid extracts. Herein, we extended shotgun lipidomics to the characterization and quantitation of cerebroside molecular species in biological samples. By exploiting the differential fragmentation patterns of chlorine adducts using electrospray ionization (ESI) tandem mass spectrometry, hydroxy and nonhydroxy cerebroside species are readily identified. The hexose (either galactose or glucose) moiety of a cerebroside species can be distinguished by examination of the peak intensity ratio of its product ions at *m/z* 179 and 89 (i.e., 0.74 ± 0.10 and 4.8 ± 0.7 for galactose- and glucose-containing cerebroside species, respectively). Quantitation of cerebroside molecular species (as little as 10 fmol) from chloroform extracts of brain tissue samples was directly conducted by 2D ESI/MS after correction for differences in ^{13}C-isotopomer intensities. This method was demonstrated to have a greater than 1,000-fold linear dynamic range in the low concentration region; therefore, it should have a wide range of applications in studies of the cellular sphingolipid lipidome.**—Han, X., and H. Cheng. **Characterization and direct quantitation of cerebroside molecular species from lipid extracts by shotgun lipidomics. *J. Lipid Res.* 2005.** 46: **163–175.**

Supplementary key words electrospray ionization • galactosylceramide • glucosylceramide • intrasource separation • sphingolipids • spinal cord • two-dimensional mass spectrometry

Cerebrosides are a family of glycosphingolipids, which are composed of a hexose and a ceramide moiety that usually consists of a long-chain amino alcohol generally referred to as a "sphingoid base" (e.g., sphingosine and sphinganine) and an amide-linked long-chain fatty acid (**Fig. 1A**) (1). Cerebrosides mediate diverse biological processes, among them the regulation of cell growth, protein trafficking and sorting, modulation of cell adhesion, formation and stabilization of axonal branches, and cell morphogenesis (see 2, 3 for recent reviews). In mammals, galactose and glucose are the main hexoses in cerebrosides, called galactocerebroside or galactosylceramide (GalCer) and glucocerebroside or glucosylceramide (GlcCer), respectively (4, 5).

GalCer species are highly enriched in brain tissues (6, 7) and constitute almost 30% of the lipid mass content of the myelin sheath (8). A GalCer-deficient transgenic mouse line has been generated by deleting the key enzyme for GalCer biosynthesis (9, 10). These mice demonstrate abnormal axonal function, dysmyelinosis, and loss of conduction velocity of axons and generally die by 3 months of age (9–11). In contrast, increased levels of GalCer, attributable to a galactosylceramidase deficiency, are responsible for globoid cell leukodystrophy (i.e., Krabbe's disease) (12, 13). GlcCer species are present in Gaucher's tissues, such as spleen, liver, lungs, bone marrow, and brain (4, 14). Although the mass content of GlcCer (as the metabolic intermediates of gangliosides) compared with GalCer in normal nerve tissues is minor (15), GlcCer levels are dramatically increased in the nervous systems of patients with Gaucher's disease (14). Accumulation of GlcCer, caused by the deficiency of a lysosomal acid β-glucosidase (i.e., glucocerebrosidase), is responsible for Gaucher's disease (14). Therefore, determination of cerebroside content and analysis of its molecular species have direct clinical relevance and applications (12, 14, 16).

Traditionally, analysis of cerebrosides from biological samples has generally depended upon the isolation of alkali-sta-

Manuscript received 23 August 2004 and in revised form 12 October 2004.

Published, JLR Papers in Press, October 16, 2004.
DOI 10.1194/jlr.D400022-JLR200

Abbreviations: 2D, two-dimensional; ESI, electrospray ionization; GalCer, galactosylceramide; GlcCer, glucosylceramide; MS/MS, tandem mass spectrometry; N18:0-d35, perdeuterated *N*-octadecanoyl; NL, neutral loss; Nm:n, the acyl amide chain of cerebroside molecular species containing m carbons and n double bonds; 2OH, 2-hydroxy.

[1] To whom correspondence should be addressed.
e-mail: xianlin@wustl.edu

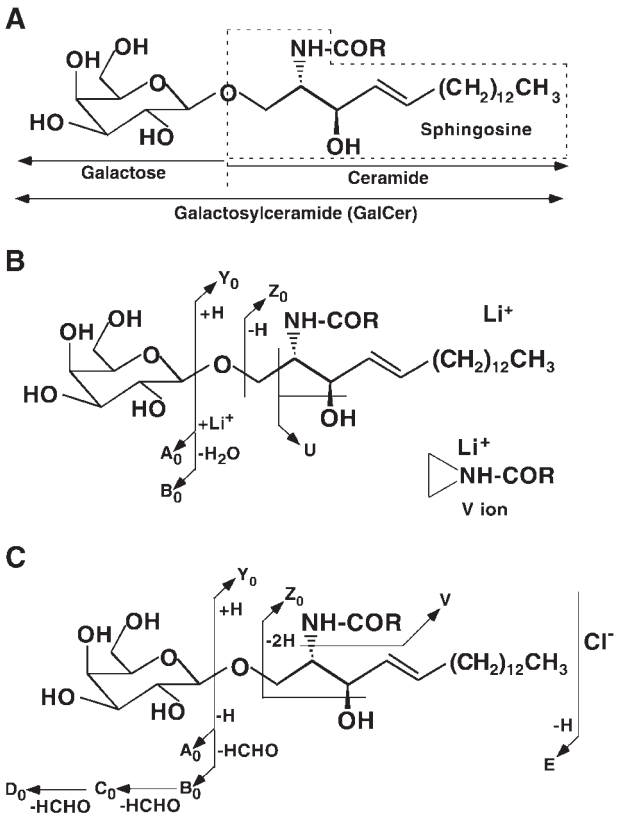

Fig. 1. The structure and designations of fragment ions of galactosylceramide (GalCer). A: Structure of GalCer and its relationship with other metabolites. B: Positive-ion fragmentations of lithium adducts of GalCer. C: Negative-ion fragmentations of chlorine adducts of GalCer. A common nomenclature system for the designation of fragment ions (21) was used.

ble glycolipids from lipid extracts followed by protection, derivatization, and quantitation of fatty acyl amide derivatives by gas chromatography or with coupling to MS (15, 17). However, this process is labor-intensive and yields results with relatively low detection sensitivity and multiple propagated errors. Total cerebroside content in biological samples has also been quantified by using multiple steps of TLC before densitometric analysis (18). Recently, many advanced analytical tools, including high performance TLC, HPLC, and several types of soft ionization MS, have been used to analyze cerebroside species after prior purification of cerebrosides from the lipid extracts of biological samples (12, 19–30).

Although we were able to analyze and quantitate major GalCer molecular species directly from the lipid extracts of biological samples by electrospray ionization (ESI)/MS without prior purification techniques (6, 7), the analysis and quantitation of many low-abundance molecular species of GalCer by this method were quite challenging. In addition, many GalCer molecular species overlap with some molecular species of choline glycerophospholipid or sphingomyelin ^{13}C-isotopomers, so the accuracy of quantitative analysis of GalCer molecular species directly from crude lipid extracts using pseudomolecular ion comparisons was relatively low (~10%).

ESI/MS has now been widely used to directly quantitate molecular species of many classes in lipid extracts of biological samples within acceptable experimental error (i.e., ≤5%) (see 31–35 for recent reviews). However, whether similar strategies using ESI/MS can be used to directly quantitate cerebroside molecular species from crude lipid extracts without prior chromatographic purification of cerebroside fractions to a higher accuracy than that demonstrated in our previous work (6, 7) requires further investigation. In addition, identification of the cerebroside hexose moiety to distinguish galactose- from glucose-containing species needs to be further explored. Although product-ion ESI/MS analyses were able to identify the 2-hydroxy (2OH) GalCer molecular species (30), effective identification of nominal isobaric molecular species of 2OH GalCer- and GalCer-containing acyl amides with an odd carbon number and one fewer double bond also needs to be established.

Very recently, we have developed a two-dimensional (2D) ESI/MS technique (36) that is an arrayed analysis by integration of both mass spectrometric and tandem mass spectrometric analyses. The first dimension of each 2D mass spectrum consists of the primary (molecular or pseudomolecular) ions in an axis of *m/z*, and its second dimension consists of the building blocks (i.e., polar head groups and/or aliphatic chains) of lipids [which are characterized by either neutral loss (NL) scans or precursor-ion scans or both] in an axis of mass (in the case of NL scanning) or *m/z* (in the case of precursor-ion scanning). By this technique, peak assignments can be substantiated by multiple independent mass spectrometric criteria, isobaric molecular species and regiospecificity can be discriminated, and quantitation of low-abundance molecular species can be performed and/or refined. Accurate quantitation of the minor pseudomolecular ions can be achieved by 2D MS analysis with a two-stage process. First, the abundant pseudomolecular ions in a selected class are quantitated by comparisons with a selected internal standard in the first-dimensional mass spectrum. Next, these values are used as endogenous standards for ratiometric comparisons to quantitate the low-abundance individual molecular species content from the subsequent tandem mass spectra.

Herein, we extend this technique to characterize and quantitate individual cerebroside molecular species directly from chloroform extracts of biological samples. Specifically, major cerebroside molecular species can be quantitated by direct comparison of the individual cerebroside ion peak intensities with that of the selected internal standard after correction for differences in ^{13}C-isotopomer intensities in both positive- and negative-ion ESI/MS analyzed as the lithium and chlorine adducts, respectively. Then, a tandem mass spectrum obtained from the NL of 162.1 u (unified atomic mass) (see Y_0 ion in Fig. 1B) from lithiated molecular ions in positive-ion mode can be used to identify all molecular species of cerebroside and quantitate/refine the minor cerebroside molecular species using the already quantified major cerebroside species as standards in addition to the original internal standard. Similarly, a tandem mass spectrum obtained from the NL of 36.0 u (corresponding to HCl) from chlorine adducts of

cerebroside molecular ions in negative-ion mode can be used to identify all molecular species of cerebroside and quantitate/refine the minor cerebroside molecular species using the previously quantified major cerebroside species as standards in addition to the original internal standard. In addition, analysis of the fragment pattern of the chlorine adduct of a cerebroside molecular species can be used to identify the hexose moiety and acyl amide moiety with or without the hydroxyl group of a cerebroside. Collectively, this study extends the 2D ESI/MS technique to profile and quantitate cerebrosides (in general) directly from a lipid extract of a biological sample and contributes a great deal to the emerging field of shotgun lipidomics.

MATERIALS AND METHODS

Materials

Semisynthetic GalCers including *N*-octadecanoyl (N18:0 GalCer) and *N-cis*-15-tetracosenoyl (N24:1 GalCer) were purchased from Sigma-Aldrich (St. Louis, MO). Semisynthetic perdeuterated *N*-octadecanoyl (N18:0-d35) GalCer, bovine brain GalCer, bovine brain hydroxy GalCer, and human spleen GlcCer were purchased from Matreya, Inc. (Pleasant Gap, PA). The purity of all semisynthetic GalCer species was determined by ESI/MS before use in quantitative analysis, and it was found that N18:0-d35 GalCer from Matreya contained ~30% of d34 deuterated *N*-octadecanoyl GalCer (**Figs. 2**, **3**). All solvents used for sample preparation and for mass spectrometric analysis were obtained from Burdick and Jackson (Honeywell International, Burdick and Jackson, Muskegon, MI). Other reagents were of analytical grade and were from Sigma-Aldrich.

Preparation of the mixtures of cerebroside molecular species

A stock solution of each GalCer or GlcCer sample in chloroform-methanol (2:1, v/v) was prepared and stored under nitrogen at −20°C. The solutions were brought to room temperature just before use. The mixtures of GalCer molecular species were prepared from these stock solutions using gas-tight syringes. The concentration of each GalCer molecular species in the mixtures ranged from 1 to 1,000 nM. The concentration of N18:0-d35 Gal-

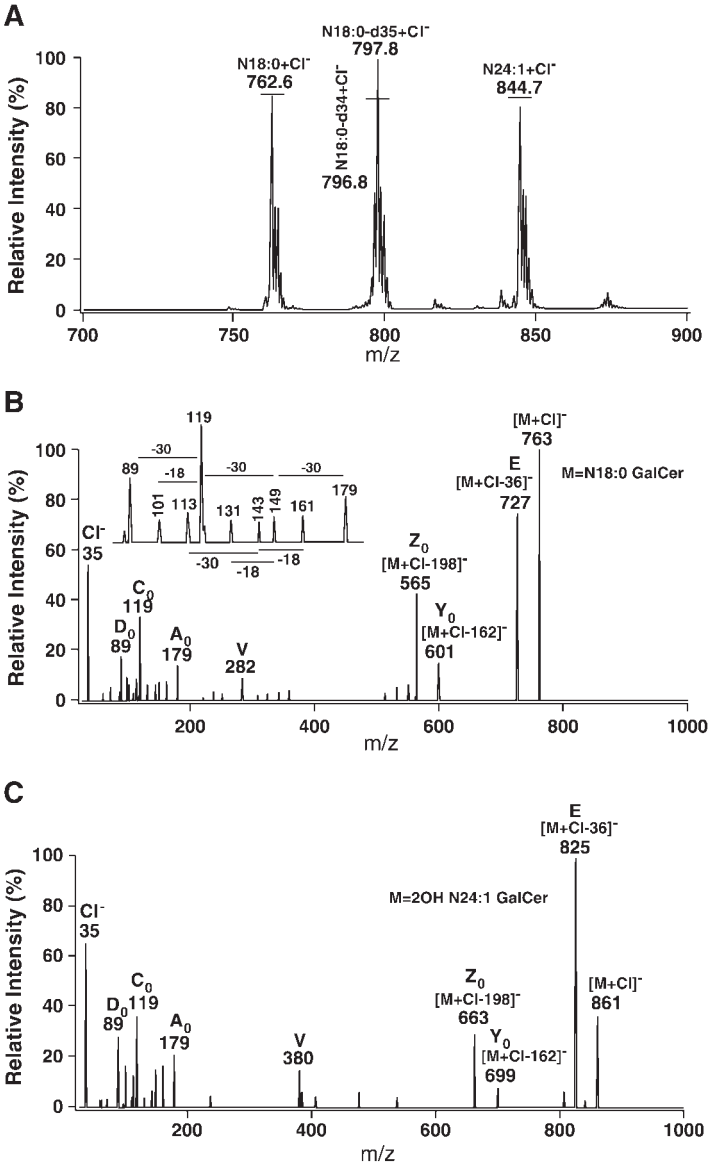

Fig. 2. A typical negative-ion electrospray ionization (ESI) mass spectrum of an equimolar mixture of GalCer and product-ion ESI mass spectra of chlorine adducts of GalCer molecular species. A: Negative-ion ESI mass spectrum of an equimolar mixture of nonhydroxy GalCer molecular species. B: Product-ion ESI mass spectrum of the chlorine adduct of N18:0 GalCer. C: Product-ion ESI mass spectrum of the chlorine adduct of 2-hydroxy N24:1 GalCer. An equimolar mixture of GalCer molecular species [i.e., N18:0, perdeuterated *N*-octadecanoyl (N18:0-d35), and N24:1 GalCer; 10 nM each in a total volume of 200 μl] was prepared and extracted as described in Materials and Methods. The solution of GalCer mixture in chloroform-methanol (1:1, v/v) was directly infused into the ESI ion source using a Harvard syringe pump at a flow rate of 2 μl/min. The chlorine adduct of hydroxy N24:1 GalCer was selected from the ESI/MS analysis of a bovine brain hydroxy GalCer mixture, which was diluted from a stock solution of bovine brain hydroxy GalCer and extracted by a modified method of Bligh and Dyer (37) in the presence of 20 mM LiCl in the aqueous phase, as described in Materials and Methods. All molecular ions in the negative-ion mass spectrum (A) were indicated after identification by product-ion ESI tandem mass spectrometry (MS/MS). The horizontal lines on or above each peak in A indicate the peak intensities after correction for ^{13}C-isotopomer differences.

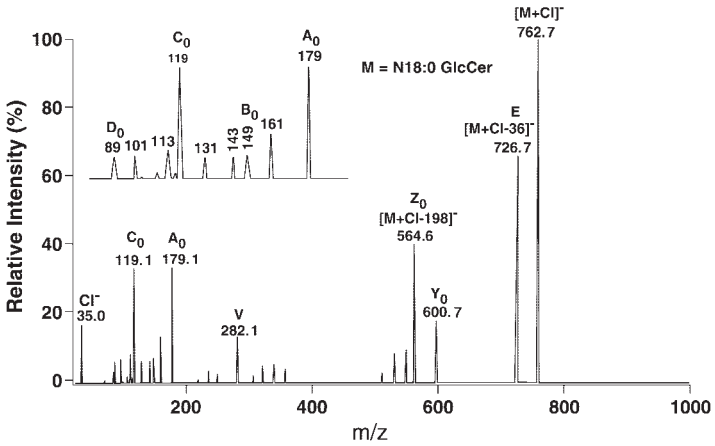

Fig. 3. A typical product-ion ESI mass spectrum of the chlorine adduct of N18:0 glucosylceramide (GlcCer). After selection of the chlorine GlcCer adduct in the first quadrupole, collisional activation was performed in the second quadrupole and the resultant product ions were analyzed in the third quadrupole as described in Materials Methods. The chlorine adduct of N18:0 GlcCer was selected from the ESI/MS analysis of a human spleen GlcCer mixture, which was diluted from a stock solution of human spleen GlcCer and extracted by a modified method of Bligh and Dyer (37) in the presence of 20 mM LiCl in the aqueous phase, as described in Materials and Methods.

Cer in its mixture with other GalCer molecular species represents only the d35 species (i.e., other deuterated species such as N18:0-d34 GalCer were not counted in the N18:0-d35 GalCer concentration of the mixture). Because sodium ions could complicate the ESI mass spectra of cerebroside and interfere with the quantitative analyses of cerebroside molecular species, all of the mixed solutions were back-extracted at least three times by a modified Bligh and Dyer technique (37) using 20 mM LiCl in an aqueous layer to minimize the presence of sodium ion in the solutions. The advantages of using LiCl in sample preparation and mass spectrometric analyses in shotgun lipidomics have recently been discussed in detail (32). The extracts were dried under a nitrogen stream, dissolved in chloroform, filtered with 0.2 μm Gelman acrodisc CR PTFE syringe filters (Gelman Science, Ann Arbor, MI), and dried under a nitrogen stream. The dried cerebroside mixtures were resuspended in 0.2 ml of chloroform-methanol (1:1, v/v) before ESI/MS analysis. This procedure minimizes the effects of sodium ions and provides sufficient lithium ions for analysis of cerebrosides by ESI/MS.

Preparation of lipid extracts from rat brain tissues

Male Sprague-Dawley rats (350–450 g body weight) were purchased from Charles River Laboratories (Wilmington, MA) and killed. Brain tissues were dissected, and ~10 mg of dissected tissue samples was homogenized in 1 ml of ice-cold PBS with a glass tissue grinder. Protein assays were performed on each of the individual homogenates. Next, lipids from another ~10 mg of dissected tissue were extracted three times by a Folch method (38) in the presence of N18:0-d35 GalCer (20 nmol/mg protein) (used as an internal standard for cerebroside quantitation). The extracts were then back-extracted three times by a modified Bligh and Dyer technique (37) using 20 mM LiCl. The lipid extracts were dried under a nitrogen stream, dissolved in chloroform, filtered with 0.2 μm Gelman acrodisc CR PTFE syringe filters (Gelman Science), reextracted, and dried under a nitrogen stream. The final lipid residue was resuspended in 1 ml of chloroform-methanol (1:1, v/v) for ESI/MS analyses.

ESI/MS of cerebrosides

ESI/MS analyses of cerebrosides were similarly performed using a Finnigan TSQ Quantum Spectrometer equipped with an electrospray ion source as described previously for the analysis of hepatic lipids (36). Typically, a 1 min period of signal averaging in the profile mode was used for each spectrum of a given cerebroside sample or lipid extract. Lipid extract samples were appropriately diluted in chloroform-methanol (1:1, v/v) before direct infusion into the ESI chamber using a syringe pump at a flow rate of 2 μl/min. Tandem mass spectrometry (MS/MS) of cerebrosides after ESI was performed by selective passage of the pseudomolecular ion(s) of cerebrosides from the first quadrupole into the second quadrupole, where dissociation was induced through collisional activation with nitrogen gas. The resultant product ions were analyzed after passage into the third quadrupole. The degree of collisional activation was adjusted through variation of the DC-offset voltage with a collision gas pressure of 1 mTorr. During this study, a collision energy of 30 eV in negative-ion mode or 50 eV in positive-ion mode was used. Two types of ESI/MS/MS (i.e., product ion and NL) were performed. Product-ion MS/MS was similarly conducted as described previously (39). The negative-ion MS/MS in NL mode was performed by coordinately scanning both the first and third quadrupoles with a mass difference (i.e., NL) of 36.0 u, corresponding to the NL of a hydrogen chloride molecule from chlorine adducts of cerebroside molecular species, whereas collision activation was performed in the second quadrupole. The positive-ion MS/MS by NL of 162.1 or 210.1 u, corresponding to the NL of galactose/glucose derivatives from lithiated cerebroside molecular species, was similarly performed.

Quantitation of cerebroside molecular species and miscellaneous

Major cerebroside molecular species were directly quantitated by comparisons of ion peak intensities with that of an internal standard (i.e., N18:0-d35 GalCer) from the first-dimensional mass spectrum after correction for the different ^{13}C-isotopomer intensities of cerebroside molecular species relative to the internal standard in either positive- or negative-ion mode (32, 40, 41). By using these previously quantified major cerebroside molecular species as a set of standards in addition to the original internal standard (i.e., N18:0-d35 GalCer), minor cerebroside molecular species were quantitated/refined by MS/MS in a 2D mass spectrometric manner as previously described (36). Quantitative data from biological samples were normalized to the protein content of the tissues, and all data are presented as means ± SD of samples from a minimum of six separate animals. Protein concentration was determined with a BCA protein assay kit (Pierce, Rockford, IL) using BSA as a standard.

RESULTS AND DISCUSSION

ESI/MS of cerebroside molecular species and identification of GalCer and GlcCer molecular species using ESI/MS/MS in negative-ion mode

To determine the utility of ESI/MS analysis of cerebroside molecular species, ion patterns of a known GalCer

mixture were characterized in negative-ion mode in initial experiments (Fig. 2). Negative-ion ESI mass spectra of an equimolar mixture of N18:0, N18:0-d35, and N24:1 GalCer (10 nM each) displayed three pseudomolecular ions at *m/z* 762.6, 797.8, and 844.7 with essentially identical intensities after correction for the different ^{13}C-isotopomer intensities of GalCer molecular species relative to the internal standard (32, 40, 41) (Fig. 2A, horizontal lines). It should be noted that the type II ^{13}C-isotopomer distribution (32, 40, 41) of N18:0-d34 GalCer contributed ~18% to the total peak intensity of N18:0-d35 GalCer in Fig. 2A. Product-ion analyses showed that these pseudomolecular ions corresponded to the chlorine adducts of GalCer species (i.e., $[M + Cl]^-$) (Fig. 2B, C). Although chlorine adducts of GalCer molecular species have not been previously characterized by ESI/MS, chlorine adducts of several other classes of lipids have been extensively studied (39, 42). The presence of the abundant isotopomer ion peaks at M + 2 in the spectra evidently suggests the ready formation of chlorine adducts of these GalCer molecular species under the experimental conditions used.

After collisional activation of a selected chlorine adduct of GalCer, multiple product ions were detected, each providing salient structural information (Fig. 1C). First, an abundant ion ($[M + Cl - 36]^-$) (the loss of HCl; E ion) and an abundant product ion at *m/z* 35 were present in each spectrum (Fig. 2B, C). These product ions indicated the presence of a chloride in the selected pseudomolecular ion. Interestingly, the peak intensity ratio of the product ion at $[M + Cl - 36]^-$ to the pseudomolecular ion (i.e., $[M + Cl]^-$) was more than 3-fold greater in production ESI mass spectra of chlorine adducts of 2OH GalCer molecular species (Fig. 2C) compared with that generated from chlorine adducts of nonhydroxy GalCer species (Fig. 2B). This feature was consistently present for all examined 2OH and nonhydroxy GalCer molecular species, indicating that the presence of the 2-hydroxyl group promotes the loss of hydrogen chloride. We speculate that this is most likely attributable to the proximity of the chlorine ion to the carbon adjacent to the amide group and the inducing effect of the hydroxyl of 2OH GalCer species causing the proton on the amide to be more acidic, thus promoting the loss of HCl. This serendipitous feature has proven to be very useful for the identification of 2OH GalCer species (see below).

Second, an abundant ion ($[M + Cl - 198]^-$; Z_0) was present. The presence of this product ion, in conjunction with the presence of a cluster of peaks between *m/z* 89 and 179 (i.e., $A_0 - D_0$ ions; Fig. 1C), characterized the galactosyl group in the selected molecular ions. A number of abundant product ion peaks between *m/z* 89 and 179 in the tandem mass spectra of chlorine GalCer adducts (Fig. 2B, C) fingerprint the fragmentation of galactose anion (*m/z* 179) with the loss of 30 (formaldehyde) and/or 18 (water) to different degrees (Fig. 2B, inset).

Finally, a unique product ion (v; Fig. 1C) was present in the product-ion ESI mass spectrum of each pseudo-GalCer molecular ion. For instance, a distinct product ion at *m/z* 282 or 380, corresponding to stearoyl amide or 2OH nervonoyl amide, respectively, was present in the negative-ion ESI tandem mass spectra of chlorinated N18:0 GalCer (Fig. 2B) or 2OH N24:1 GalCer (Fig. 2C), respectively. Therefore, the acyl amide substituents of GalCer molecular species can be readily identified from the characterization of this product ion.

GlcCer molecular species are mutually isobaric with their GalCer counterparts. Previously, ESI/MS/MS/MS or source-induced dissociation followed by MS/MS of lithiated cerebrosides was used to identify the hexose moiety (30). In this study, we found that these hexose moieties could be much more readily identified by negative-ion ESI/MS/MS of their chlorine adducts. For example, Fig. 3 shows a product-ion ESI mass spectrum of chlorine N18:0 GlcCer adduct. By comparison of the fragment ion patterns between N18:0 GlcCer (Fig. 3) and N18:0 GalCer (Fig. 2B), the only apparent difference between the spectra is the intensity ratio of product ions at *m/z* 179 vs. 89. The average intensity ratios of this pair of product ions are 0.74 ± 0.10 and 4.8 ± 0.7 for GalCer and GlcCer molecular species, respectively, as obtained from the analysis of more than 10 different molecular species of each subclass. We speculate that these different ratios result from the different stabilities of the fragments from the anionic hexoses of GalCer and GlcCer species caused by differences in their hexose configurations. These ratios can be used to clearly distinguish GlcCer from GalCer molecular species and to assess the composition of each component in a GlcCer and GalCer mixture. Of course, it becomes impractical to identify a component based on this criterion when this component is only minor in the mixture. In addition, only the fragmentation patterns of GalCer and GlcCer species have been examined in this study. If one were interested in cerebrosides containing other hexose moieties, the fragmentation patterns of those cerebrosides should be further characterized.

ESI/MS of GalCer molecular species and identification of GalCer molecular species using ESI/MS/MS in positive-ion mode

Positive-ion ESI mass spectra of an equimolar mixture of N18:0 GalCer, N18:0-d35 GalCer, and N24:1 GalCer (10 nM each) under experimental conditions similar to those of negative-ion ESI/MS displayed two sets of pseudomolecular ion peaks, one at *m/z* 734.6, 769.8, and 816.7 and another at *m/z* 750.6, 785.8, and 832.7 (**Fig. 4A**). The abundance of each set of ion peaks was almost identical within experimental error after correction for the different ^{13}C-isotopomer intensities of GalCer molecular species relative to the internal standard (32, 40, 41) (as indicated with horizontal lines). The more intense set (i.e., *m/z* 734.6, 769.8, and 816.7) represented lithium adducts of GalCer species, whereas the lower abundance set represented sodium GalCer adducts. The sodiated GalCer molecular ions were consistently present in the positive-ion ESI mass spectra, even after the mixture was back-extracted four times by the modified method of Bligh and Dyer (37) in the presence of 20 mM LiCl. This observation suggests that sodium ions tightly bind cerebrosides

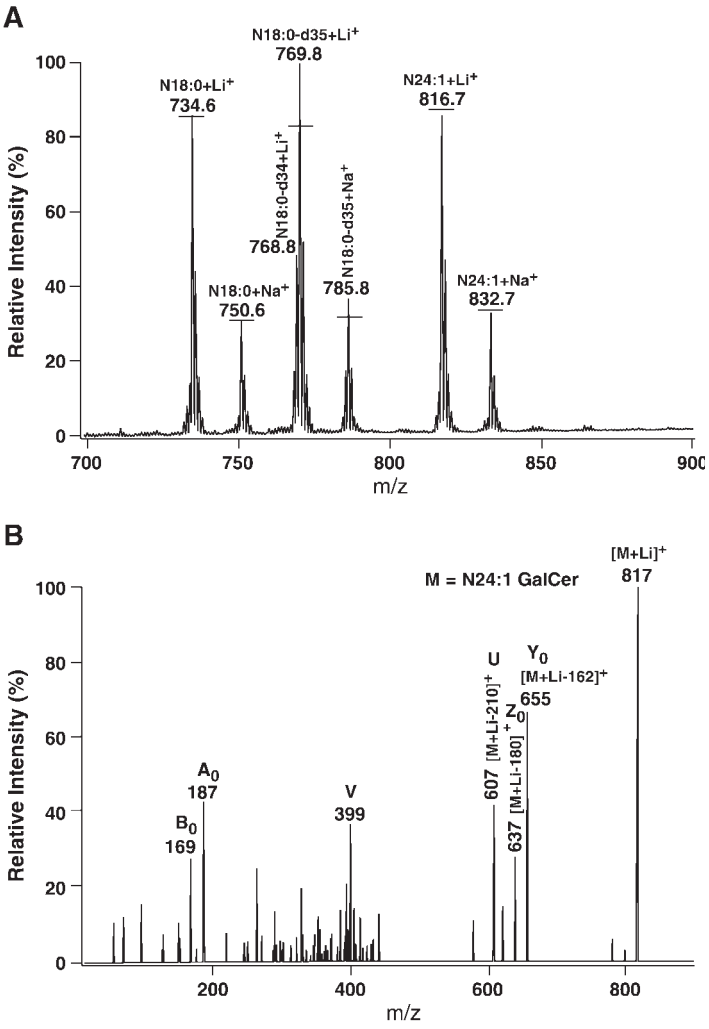

Fig. 4. A typical positive-ion ESI mass spectrum of an equimolar mixture of galactocerebrosides and a product-ion ESI mass spectrum of lithium galactocerebroside adduct. A: Positive-ion ESI mass spectrum of an equimolar mixture of GalCer molecular species. B: Product-ion ESI mass spectrum of the lithium adduct of N24:1 GalCer. Sample preparation, positive-ion mass spectrometry, and MS/MS of GalCer were performed as described for Fig. 2. The horizontal lines on or above each peak in A indicate the peak intensities after correction for ^{13}C-isotopomer differences.

and/or are readily available under the experimental conditions used.

Selection and collisional activation of the lithium adduct yielded three types of product ions (Fig. 1B) similar to those previously described (30). The first type of product ions were all related to the NL of galactosyl head groups and were present in all ESI tandem mass spectra of lithium GalCer adducts (Fig. 4B). These product ions included $[M + Li - 162]^+$ (Y_0), $[M + Li - 180]^+$ (Z_0), and $[M + Li - 210]^+$ (U). The second type of product ions were at *m/z* 187 (A_0) and 169 (B_0) (Fig. 4B). The third type of product ions carried structural information about aliphatic chains in the GalCer molecular species. For example, there was an abundant product ion at *m/z* 399 in tandem mass spectra of the lithium adduct of N24:1 GalCer (Fig. 4B), corresponding to the V ion (Fig. 1B). There were other numerous minor product ion peaks around this region derived from either loss of the aliphatic constituent from the sphingosine base or loss of fatty acyl amide derivatives. Selection and collisional activation of the lithium adduct of 2OH GalCer in positive-ion mode yielded essentially an identical product ion pattern to that previously described (30).

Positive-ion ESI/MS/MS of sodium adducts of GalCer molecular species showed identical product ions but with altered abundance (spectra not shown). Product ions $[M + Na - 162]^+$, $[M + Na - 180]^+$, and $[M + Na - 210]^+$, in particular the last one, derived from the sodium adducts of GalCer, were at least 50% lower in relative abundance compared with those derived from the lithium adducts of GalCer. These results suggest different interactions of the head group region of GalCer with sodium ion and lithium ion. Furthermore, instead of the lithiated galactose and its derivative at *m/z* 187 and 169 in the tandem mass spectra of lithiated GalCer, a sodiated galactose and its derivative at *m/z* 203 and 185 were present in the ESI tandem mass spectra of sodiated GalCer (data not shown). These features were readily used to distinguish sodium adducts of GalCer molecular species from lithium adducts of hydroxy GalCer molecular species that could be located at nominal isobaric peaks.

Quantitation of GalCer molecular species

ESI/MS analyses of equimolar mixtures of GalCer molecular species in both negative- and positive-ion modes displayed essentially identical peak intensities after correction for the different ^{13}C-isotopomer intensities of GalCer molecular species relative to the internal standard (32, 40, 41)

(Figs. 2A, 4A, horizontal lines). Although the ^{37}Cl-isotopomer effects make the quantitation of GalCer molecular species more difficult using negative-ion ESI/MS, analysis of GalCer molecular species by negative-ion ESI/MS was not complicated by the nominal isobaric peaks resulting from sodiated nonhydroxy GalCer and lithiated hydroxy GalCer as in the positive-ion ESI/MS of GalCer. Therefore, GalCer molecular species can be redundantly quantitated by both negative- and positive-ion ESI/MS. It should be noted that the location of double bond(s) in acyl amide chains could not be identified in this study; therefore, the isobaric molecular species attributable to the difference in the double bond location of acyl amide were not resolved and quantitated.

To assess the accuracy of quantitative analysis of cerebroside molecular species by ESI/MS, two additional experiments were performed. First, equimolar mixtures of N18:0 GalCer, N18:0-d35 GalCer, and N24:1 GalCer, in which the concentration ranged from 1 to 1,000 nM for each individual GalCer component, were prepared. Both negative- and positive-ion ESI/MS analyses demonstrated almost identical molecular ion abundance (within experimental error) after correction for different isotopomer distributions for all samples prepared (spectra not shown). The results demonstrate that the linear dynamic range of cerebroside quantitation by either negative- or positive-ion ESI/MS analysis is greater than 1,000-fold in this low concentration range. Second, a set of mixtures of N18:0-d35 GalCer with N18:0 GalCer and N24:1 GalCer at different molar ratios and different concentrations was prepared. Upon examination of peak intensity ratios of these mixtures in both negative- and positive-ion ESI/MS, a linear correlation between the prepared molar ratios in the mixture and the ion peak intensity ratios after correction for ^{13}C-isotopomer intensity differences was demonstrated (**Fig. 5**). A correlation coefficient of 0.995 or 0.993 and a slope of 1.06 or 1.08 from the mixtures of N18:0 GalCer or N24:1 GalCer with N18:0-d35 GalCer, respectively, were documented (Fig. 5) by positive-ion ESI/MS. A similar result was also obtained from the utility of negative-ion ESI/MS (data not shown). These results demonstrate that a 100-fold linear dynamic range using an internal standard to directly quantitate cerebroside molecular species of interest by either negative- or positive-ion ESI/MS is promising. It should be noted that an optimal molar ratio between the species of interest and the internal standard used is between 0.2 and 0.8. Beyond this range, significant experimental errors could be induced, depending on factors such as baseline drift (i.e., chemical noise) and ion peak intensity fluctuation (i.e., instrumental stability). However, most of these factors can be eliminated by ESI/MS/MS analysis with NL scanning, and minor cerebroside molecular species can be refined by the 2D ESI/MS approach (see below), by which quantitation of minor peaks (e.g., peak intensities that are <1% of the most abundant peak of a cerebroside molecular species) can be readily achieved. This represents a greater than 1,000-fold dynamic range of quantitation relative to a selected internal standard because the measurement of concentrations under the experimental conditions is dynamically linear, as demonstrated above.

Quantitative analyses of cerebroside molecular species using 2D ESI/MS

Studies of the acquired ESI mass spectra of brain tissue extracts consistently demonstrated some overlap of lithiated

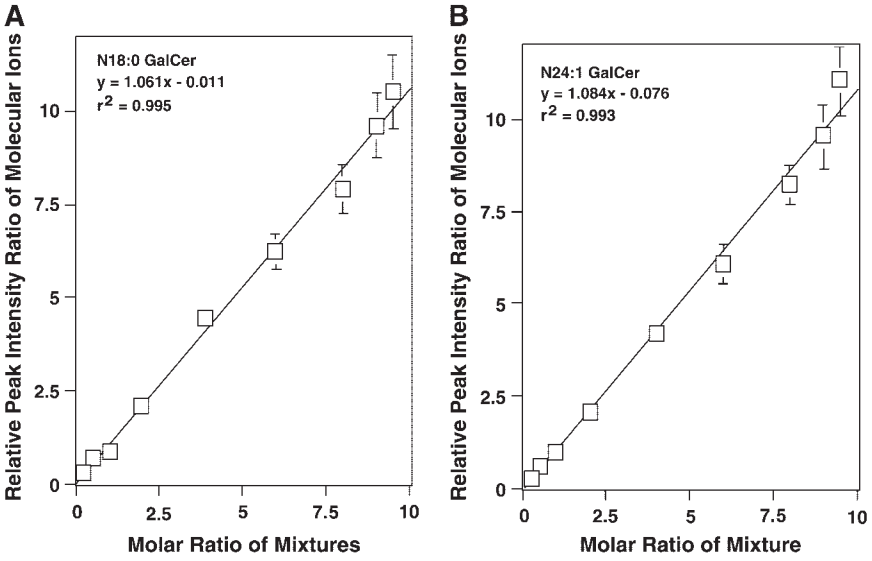

Fig. 5. Correlation of the determined peak intensity ratios relative to internal standards from mass spectra with the expected molar ratio in the mixture. Mixtures of N18:0 (A) and N24:1 (B) GalCer molecular species containing differential molar ratios relative to N18:0-d35 GalCer (used as an internal standard) with concentrations ranging from 1 to 1,000 nM for each GalCer component were prepared as described in Materials and Methods. The lithiated ion peak intensity ratios of N18:0 and N24:1 GalCer molecular species relative to the N18:0-d35 GalCer ion peak were determined from the positive-ion ESI/MS analyses after corrections for ^{13}C-isotopomer differences. The correlation coefficient (r^2) and slope of the linear plots are as indicated for both molecular species. Data are presented as means ± SEM from at least four separate sample preparations.

GalCer molecular ions with choline glycerophospholipids in positive-ion ESI spectra or overlap of chlorine GalCer adducts with sulfatide, phosphatidylserine, and/or phosphatidylinositol molecular ions in negative-ion spectra in shotgun lipidomics (6, 7, 32). Therefore, under these conditions, it was difficult to directly quantitate all of the cerebroside molecular species from brain tissue extracts only by ESI/MS. To solve this problem, isolation of the cerebroside fraction using HPLC or TLC as described previously (17, 20) can be performed before ESI/MS analysis.

Alternatively, shotgun lipidomics with a 2D ESI/MS approach can be developed, because cerebroside molecular species may be directly profiled from a lipid extract of a biological sample after the "spectrometric isolation" of cerebroside molecular species from the overlapping peaks of other lipid molecular species in the extract. Thus, in this 2D ESI/MS approach, the major and nonoverlapping ion peaks of cerebrosides are quantified in the first-dimensional mass spectra of either lithium or chlorine adducts of cerebrosides in positive- or negative-ion ESI/MS, respectively, as described above. Then, using these newly quantified major cerebroside molecular species as a set of endogenous standards in addition to the original internal standard, the mass content of other minor or overlapping ion peaks of cerebroside molecular species can be determined by linear comparisons with their neighboring standards or by development of an algorithm derived from all of the standards. It should be noted that the peaks composed of multiple isobaric molecular species should not be selected as an endogenous internal standard to minimize the effects of differential fragmentation on quantitation, as discussed previously (32).

Although MS/MS has been used to profile and/or semiquantitate multiple lipid classes directly from lipid extracts of biological samples (43–46), profiling and/or semiquantitation of cerebroside molecular species directly from lipid extracts of biological samples by MS/MS has not been developed. Analyses of product-ion ESI mass spectra of GalCer and GlcCer molecular species in either positive- (30) or negative-ion mode (see above) result in several useful NL values, for which the product ions are very abundant. For example, NL values of 162.1 and 210.1 u (see Y_0 and U ions in Fig. 1B) can be used to profile cerebroside molecular species in positive-ion mode. Similarly,

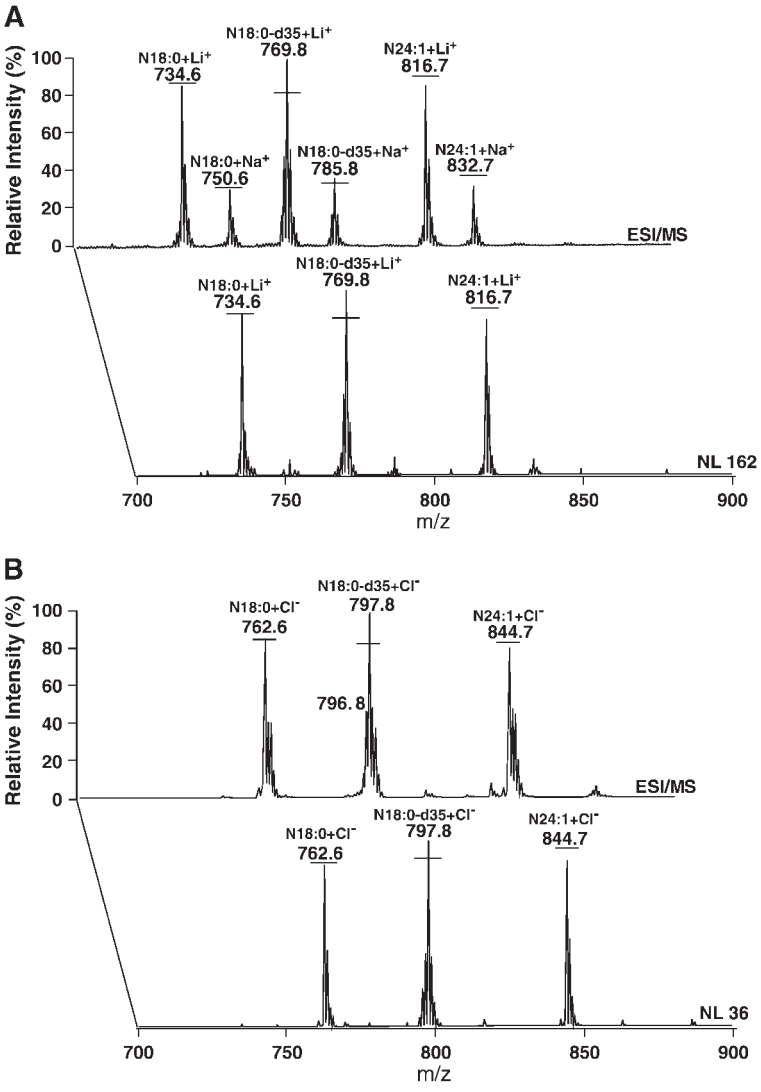

Fig. 6. Partial two-dimensional (2D) ESI mass spectra of an equimolar mixture of galactocerebrosides in positive- and negative-ion mode. An equimolar mixture of GalCer molecular species (i.e., N18:0, N18:0-d35, and N24:1 GalCer; 10 nM each) was prepared and directly infused into the ESI ion source using a Harvard syringe pump at a flow rate of 2 μl/min, as described in Materials and Methods. A: A conventional ESI mass spectrum in positive-ion mode was acquired as described for Fig. 4A before analysis in the second dimension by neutral loss (NL) of 162.1 u. Similarly, a conventional ESI mass spectrum in negative-ion mode was acquired under identical conditions to those described for Fig. 2A before analysis in the second dimension by NL of 36.0 u. B: Each NL scan was acquired by simultaneously scanning the first and third quadrupoles at a fixed mass difference (NL) at a rate of 300 u/s while the first quadrupole was scanned over *m/z* 700–900. The horizontal lines indicate the peak intensities after correction for the different ^{13}C-isotopomer intensities of GalCer molecular species relative to the internal standard.

NL of 36.0 u may be used to analyze cerebroside molecular species in negative-ion mode.

For an equimolar mixture of GalCer molecular species (identical to those used in Figs. 2, 4), positive-ion ESI tandem mass spectra with NL values of 162.1 (**Fig. 6A**) and 210.1 u (spectra not shown) and negative-ion ESI tandem mass spectra with NL of 36.0 u (Fig. 6B) were acquired. Each of three NL tandem mass spectra displayed essentially identical molecular ion intensities after correction for ^{13}C-isotopomer distributions (Fig. 6, horizontal lines). The acquired NL mass spectra of 210.1 u were essentially identical to those acquired from the NL of 162.1 u (spectra not shown). It should be noted that the sodium adducts of GalCer molecular species in the NL mass spectra were minimal and could be neglected in most cases. This was likely attributable to the combination of both the low abundance of sodiated molecular ions and the lower rates at which these fragment ions were generated from sodium GalCer adducts compared with the corresponding lithium adducts (see above). Therefore, complications (such as the coexistence of sodium GalCer adducts with lithium adducts of 2OH GalCer in a nominally isobaric peak) induced by the presence of the sodium adduct of cerebroside in mass spectrometry could be resolved through the performance of NL MS/MS. Any residual portion of sodium adduct can be subtracted from the ion peak intensity according to the ratio of other sodiated ion peaks. Furthermore, it should also be noted that the ^{37}Cl-isotope effect was no longer present in the negative-ion ESI tandem mass spectra of NL scanning for H^{35}Cl (Fig. 6B).

The developed methodology was first applied to the quantitative analyses of commercially available bovine brain GalCer. **Figure 7** partially shows both positive- and negative-ion 2D ESI mass spectra for the analyses of bovine brain GalCer with an internal standard (i.e., N18:0-d35 GalCer). Although many major GalCer molecular species could be quantitated in the first-dimensional spectra by comparison of the peak intensity of individual GalCer species with that of the selected internal standard, minor GalCer molecular ions were unable to be identified and/or quantitated because of either the presence of sodium GalCer adducts in the positive-ion mode (Fig. 7A) or the presence

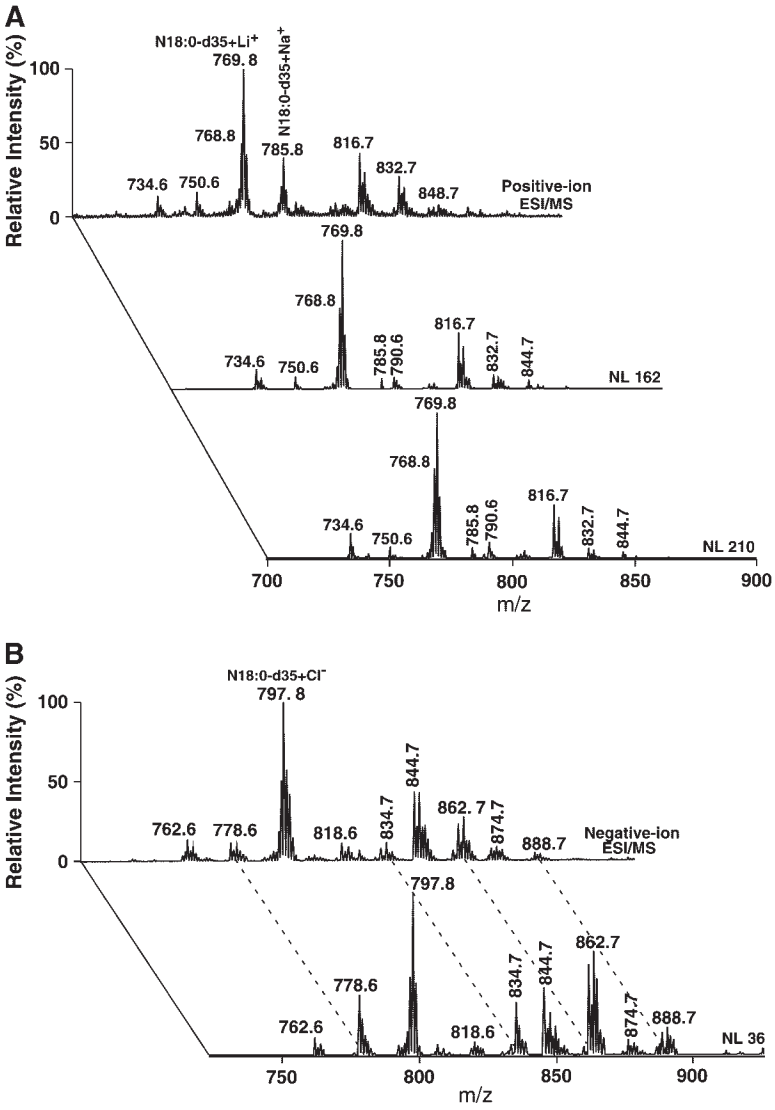

Fig. 7. 2D ESI mass spectra of bovine brain galactocerebrosides in both positive- and negative-ion mode. Bovine brain galactocerebrosides (total, 100 pmol) were mixed with an internal standard (i.e., N18:0-d35 GalCer; 50 pmol). The mixture was extracted by a modified Bligh and Dyer method (37) in the presence of 20 mM LiCl and then resuspended in 1 ml of chloroform-methanol (1:1, v/v). The solution of the GalCer mixture was directly infused into the ESI ion source using a Harvard syringe pump at a flow rate of 2 μl/min. A: A conventional ESI mass spectrum in positive-ion mode was acquired before analysis in the second dimension by NL of 162.1 or 210.1 u (unified atomic mass). B: Similarly, a conventional ESI mass spectrum in negative-ion mode was acquired before analysis in the second dimension by NL of 36.0 u. Each NL scan was acquired by simultaneous scanning of the first and third quadrupoles at a fixed mass difference (NL) at a rate of 300 u/s while the first quadrupole was scanned over the indicated *m/z* range. The broken lines in B indicate the ion clusters of hydroxy GalCer molecular species.

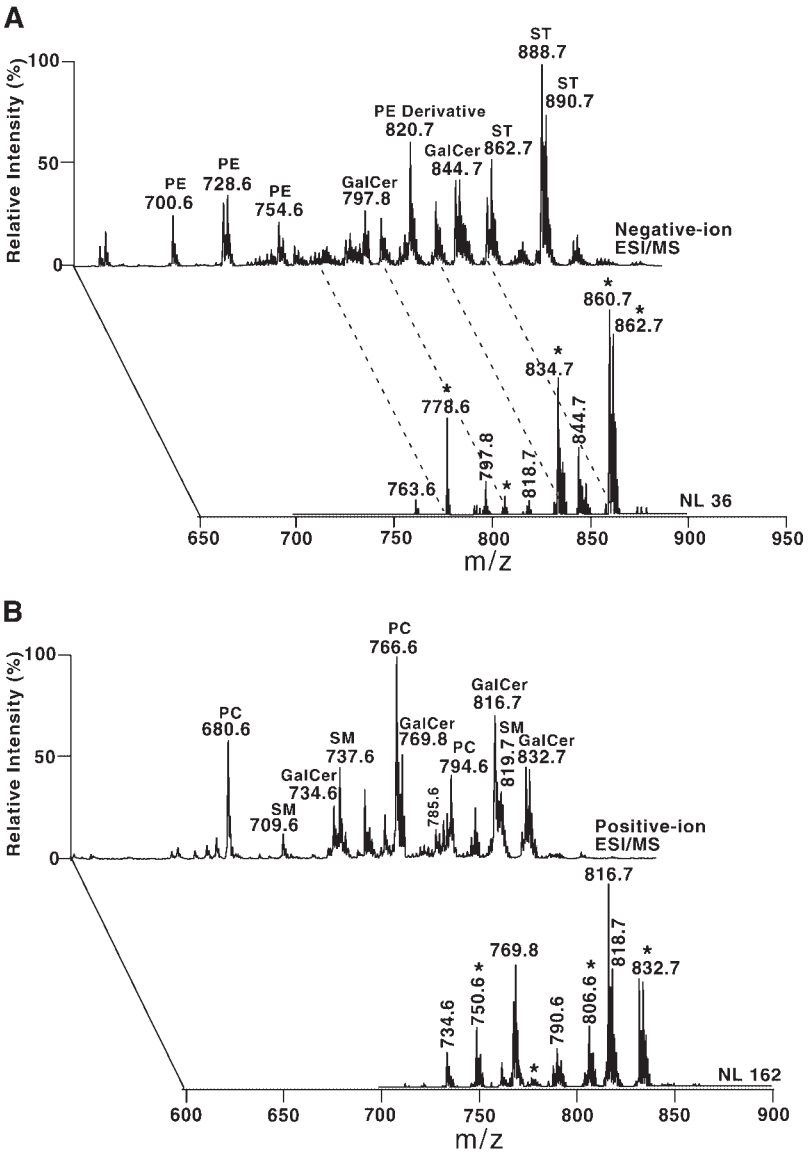

Fig. 8. Partial 2D ESI mass spectra of chloroform extracts of rat spinal cords in both positive- and negative-ion mode. Lipid samples from rat spinal cords (~10 mg of wet tissue of each) containing an internal standard (i.e., N18:0-d35 GalCer) were extracted by a Folch method (38) followed by a back-extraction using a modified Bligh and Dyer method (37) in the presence of 20 mM LiCl. Aliquots of the extracts in chloroform-methanol (1:1, v/v) containing less than 10 pmol/μl total lipids were infused directly into the ESI source using a Harvard syringe pump at a flow rate of 2 μl/min. A: A conventional ESI mass spectrum in positive-ion mode was acquired before analysis in the second dimension by NL of 162.1 u. B: Similarly, a conventional ESI mass spectrum in negative-ion mode was acquired before analysis in the second dimension by NL of 36.0 u. Each NL scan was acquired by simultaneous scanning of the first and third quadrupoles at a fixed mass difference (NL) at a rate of 300 u/s while the first quadrupole was scanned over the indicated *m/z* range. The asterisks in both A and B and the broken lines in B indicate the ion clusters of hydroxy GalCer molecular species. PC, choline glycerophospholipid; PE, ethanolamine glycerophospholipid; SM, sphingomyelin; ST, sulfatide.

of the ^{37}Cl isotope peak (Fig. 7B). Furthermore, 2OH GalCer molecular species were not yet identified in the first-dimensional spectra. Therefore, 2D ESI/MS analyses of bovine brain GalCer were performed with NL values of 162.1 and 210.1 u in positive-ion mode (Fig. 7A) and 36.0 u in negative-ion mode (Fig. 7B).

Positive-ion ESI/MS analyses using NL values of 162.1 and 210.1 u for bovine brain GalCer molecular ions demonstrated essentially identical mass spectra (Fig. 7A). These spectra were also closely analogous to the ion patterns in both the positive- and negative-ion ESI mass spectra of bovine brain GalCer (Fig. 7). Moreover, the positive-ion NL mass spectra were simplified with the minimized sodium adduct peaks of GalCer compared with their parent mass spectra (Fig. 7A). For example, the peak intensity of the ion at *m/z* 785.8 (i.e., N18:0-d35 + Na^+) was reduced from 40% in positive-ion ESI mass spectra to ~5% in tandem mass spectra of NL 162.1 and 210.1 u (i.e., a reduction of ~90%) (Fig. 7A). Peaks at *m/z* 750.6 and 832.7 represent examples of nominally isobaric peaks of sodiated GalCer ions and lithiated 2OH GalCer ions (Fig. 7A). The intensities of these peaks in the corresponding NL mass spectra were substantially lower compared with those in the positive-ion ESI/MS mass spectra (Fig. 7A). The contribution of sodiated GalCer to these peak intensities was less than 10% (as seen from the sodiated internal standard peak); therefore, it could be neglected in the quantitation of lithiated hydroxy GalCer molecular species. It should also be noted that the baselines in the tandem mass spectra were substantially improved compared with their parent mass spectra (Fig. 7A).

Negative-ion NL mass spectra of bovine brain GalCer were not complicated by the ^{37}Cl-isotopomers that were present in their parent negative-ion mass spectra (Fig. 7B). As anticipated, the negative-ion mass spectra of bovine brain GalCer with NL of 36.0 u (Fig. 7B) displayed a substantially different ion pattern compared with either positive-ion tandem mass spectra in NL mode (Fig. 7A) or both positive- and negative-ion ESI/MS mass spectra of the sample (Fig. 7). This was attributable to the dramati-

TABLE 1. GalCer content in rat spinal cord and brain tissues

GalCer	$[M + Li]^+$	Spinal Cord	Cortex White Matter	Cortex Gray Matter	Cerebellum
N18:0	734.6	6.7 ± 0.7	6.6 ± 0.6	1.1 ± 0.1	3.8 ± 0.3
2OH N18:0	750.6	9.2 ± 0.6	8.5 ± 0.2	0.6 ± 0.1	4.9 ± 0.5
N20:0	762.6	4.7 ± 0.4	3.8 ± 0.2	0.2 ± 0.1	1.2 ± 0.1
2OH N20:0	778.6	2.3 ± 0.3	2.9 ± 0.3	0.2 ± 0.1	1.1 ± 0.2
N22:1	788.6	3.5 ± 0.3	1.1 ± 0.1	0.1 ± 0.1	0.3 ± 0.1
N22:0	790.6	7.6 ± 0.5	8.8 ± 0.7	1.6 ± 0.1	3.8 ± 0.2
2OH N21:0	792.6	4.5 ± 0.4	8.7 ± 0.6	1.1 ± 0.2	4.3 ± 0.4
N23:0	804.6	2.1 ± 0.2	1.4 ± 0.1	0.3 ± 0.1	0.7 ± 0.1
2OH N22:0	806.6	9.5 ± 0.6	8.7 ± 0.1	1.9 ± 0.3	8.2 ± 0.5
N24:1	816.7	30.7 ± 3.5	26.6 ± 2.8	4.6 ± 0.4	9.2 ± 0.7
N24:0	818.7	15.8 ± 1.8	20.6 ± 2.5	2.6 ± 0.2	7.3 ± 0.5
2OH N23:0	820.7	6.3 ± 0.5	9.1 ± 0.8	0.7 ± 0.1	4.0 ± 0.4
2OH N24:1	832.7	20.2 ± 1.7	18.6 ± 1.5	1.5 ± 0.2	8.1 ± 0.7
2OH N24:0	834.7	19.0 ± 1.6	15.6 ± 1.6	2.2 ± 0.3	13.5 ± 1.6
N26:1	844.7	1.4 ± 0.2	4.3 ± 0.3	0.3 ± 0.1	1.2 ± 0.2
N26:0	846.7	0.3 ± 0.1	0.6 ± 0.1	0.6 ± 0.1	0.7 ± 0.1
Total		143.8 ± 9.3	145.9 ± 9.4	19.6 ± 2.2	72.3 ± 5.1
Total 2OH GalCer		71.0 ± 3.2	72.1 ± 4.6	8.2 ± 1.3	44.1 ± 3.2

GalCer, galactosylceramide; Nm:n, the acyl amide chain of cerebroside molecular species containing m carbons and n double bonds; 2OH, 2-hydroxy. Lipids of rat nerve samples were extracted by the Folch method (38) and back-extracted by a modified Bligh and Dyer method (37). GalCer molecular species were identified and quantified by two-dimensional electrospray ionization mass spectrometry as described in the text. The results are expressed in nmol/mg protein and represent means ± SD of lipid extracts from at least six separate animals.

cally increased loss of hydrochloride from 2OH GalCer molecular species compared with nonhydroxy GalCer molecular species (see above), whereas all chlorine adducts of nonhydroxyl GalCer molecular species showed equal ionization sensitivity, as demonstrated with the equimolar mixtures of GalCer (Fig. 6B). These substantially intensified ion peaks were present at *m/z* 778.6, 834.7, 860.7, 862.7, 886.7, and 888.7, corresponding to 2OH N18:0, 2OH N22:0, 2OH N24:1, 2OH N24:0, 2OH N26:2, and 2OH N26:1 GalCer molecular species, respectively (Fig. 7B). Therefore, all GalCer molecular species were identified in negative-ion MS/MS by a NL of 36.0 u and were quantitatively refined as their lithium adducts by positive-ion MS/MS with a NL of 162.1 or 210.1 u after major and nonoverlapping GalCer molecular species were quantitated either in positive- or negative-ion mode or both.

Quantitation of GalCer molecular species in chloroform extracts of rat brain tissues by shotgun lipidomics

Next, we applied the developed methodology to the direct quantitation of GalCer molecular species in chloroform extracts of rat spinal cord and brain tissues, including cortex gray matter, cortex white matter, and cerebellum, without prior chromatographic separation. Because the mass content of GlcCer compared with GalCer in normal nerve tissues is negligible (15), only GalCer molecular species were analyzed in this study. Initial ESI/MS analysis revealed severe overlapping of chlorine GalCer adducts with sulfatide, phosphatidylserine, and/or phosphatidylinositol molecular ions in negative-ion spectra (**Fig. 8A**) and overlapping of lithium adducts of GalCer molecular species with choline glycerophospholipids in positive-ion ESI mass spectra (Fig. 8B). Therefore, direct quantitation of all GalCer molecular species using only ESI/MS was not feasible.

These difficulties were resolved by the utility of 2D ESI/MS. First, nonhydroxy GalCer and 2OH GalCer molecular species were distinguished and identified in negative-ion 2D ESI/MS with NL scanning of 36.0 u (Fig. 8A). As anticipated, the negative-ion mass spectra of tissue extracts with NL of 36.0 u (Fig. 8A) displayed a substantially different ion pattern compared with positive-ion tandem mass spectra in NL mode (Fig. 8B). These substantially intensified ion peaks were present at *m/z* 778.6, 834.7, 860.7, and 862.7, corresponding to 2OH N18:0, 2OH N22:0, 2OH N24:1, and 2OH N24:0 GalCer molecular species, respectively (Fig. 8A). Thus, all GalCer molecular species, including hydroxy GalCer species, were identified and tabulated (**Table 1**). Next, abundance and nonoverlapping lithium adducts of GalCer species, including at *m/z* 734.6, 816.7, 818.7, 832.7, and 834.7, corresponding to N18:0, N24:1, N24:0, 2OH N24:1, and 2OH N24:0, respectively, were first quantitated in positive-ion ESI/MS by comparison of each ion peak intensity with that of the internal standard after correction for ^{13}C-isotopomer distributions (Fig. 8B, Table 1). Finally, other low-abundance GalCer molecular species were quantitated using positive-ion MS with a NL of 162.1 u (Fig. 8B, Table 1) by linear comparisons with their neighboring GalCer molecular ions (as quantified above) after correction for ^{13}C-isotopomer distributions.

ESI/MS analyses demonstrated that N24:1 GalCer was the major GalCer molecular species in all analyzed samples except cerebellum, in which 2OH N24:0 was the major GalCer species (Table 1). Hydroxy GalCer species constituted 49.3, 49.4, 41.8, and 61.0 mol% of the total GalCer present in rat spinal cord, cortex white matter, cortex gray matter, and cerebellum, respectively (Table 1). The ratios of hydroxy GalCer mass content vs. nonhydroxy GalCer mass content (i.e., ~1) in this study agree well with previous findings (7, 15, 47). The GalCer molec-

ular species profile of rat spinal cord in this study is also in close agreement with the profiles obtained using reversed-phase HPLC after separation by straight-phase HPLC (47). Both the total content and the molecular species profiles of GalCer present in spinal cord and cortex white matter were similar (Table 1). Interestingly, GalCer content was not abundant in the cortex gray matter of rat brain, suggesting that GalCer molecular species were predominantly present in myelin sheaths. The total GalCer content in rat cerebellum was approximately half of that found in rat spinal cord and cortex white matter. This likely resulted from the preparation of the samples, in which white and gray matter were not separated for cerebellum as was done for cortex.

Collectively, this report describes the identification of structural information about cerebroside molecular species, including fatty acyl amide substituents, hexose moieties, and the presence of hydroxyl groups, using ESI/MS/MS in positive- and/or negative-ion modes. Furthermore, accurate quantitation of cerebroside molecular species was achieved directly from chloroform extracts of biological samples by shotgun lipidomics based upon 2D ESI/MS. It can be speculated that this methodology will be useful for a wide range of physiological and pathological studies.

This work was supported by National Institutes of Health Grant PO-1HL57278 and by NIA Grant P50 AG05681 and the Neurosciences Education and Research Foundation. X.H. is the 2003/2004 Memory Ride Prize recipient. The authors are grateful to Drs. Christopher M. Jenkins and Kui Yang for their comments.

REFERENCES

1. Merrill, A. H., Jr., and C. C. Sweeley. 1996. Sphingolipids: metabolism and cell signalling. *In* Biochemistry of Lipids, Lipoproteins and Membranes. D. E. Vance and J. Vance, editors. Elsevier, Amsterdam. 309–339.
2. Hakomori, S. 2003. Structure, organization, and function of glycosphingolipids in membrane. *Curr. Opin. Hematol.* **10:** 16–24.
3. Bektas, M., and S. Spiegel. 2004. Glycosphingolipids and cell death. *Glycoconj. J.* **20:** 39–47.
4. Stults, C. L., C. C. Sweeley, and B. A. Macher. 1989. Glycosphingolipids: structure, biological source, and properties. *Methods Enzymol.* **179:** 167–214.
5. Tan, R. X., and J. H. Chen. 2003. The cerebrosides. *Nat. Prod. Rep.* **20:** 509–534.
6. Han, X., D. M. Holtzman, D. W. McKeel, Jr., J. Kelley, and J. C. Morris. 2002. Substantial sulfatide deficiency and ceramide elevation in very early Alzheimer's disease: potential role in disease pathogenesis. *J. Neurochem.* **82:** 809–818.
7. Han, X., H. Cheng, J. D. Fryer, A. M. Fagan, and D. M. Holtzman. 2003. Novel role for apolipoprotein E in the central nervous system: modulation of sulfatide content. *J. Biol. Chem.* **278:** 8043–8051.
8. Norton, W. T., and W. Cammer. 1984. Isolation and characterization of myelin. *In* Myelin. P. Morell, editor. Plenum Press, New York. 147–195.
9. Coetzee, T., N. Fujita, J. Dupree, R. Shi, A. Blight, K. Suzuki, and B. Popko. 1996. Myelination in the absence of galactocerebroside and sulfatide: normal structure with abnormal function and regional instability. *Cell.* **86:** 209–219.
10. Bosio, A., E. Binczek, and W. Stoffel. 1996. Functional breakdown of the lipid bilayer of the myelin membrane in central and peripheral nervous system by disrupted galactocerebroside synthesis. *Proc. Natl. Acad. Sci. USA.* **93:** 13280–13285.
11. Bosio, A., H. Bussow, J. Adam, and W. Stoffel. 1998. Galactosphingolipids and axono-glial interaction in myelin of the central nervous system. *Cell Tissue Res.* **292:** 199–210.
12. Esch, S. W., T. D. Williams, S. Biswas, A. Chakrabarty, and S. M. Levine. 2003. Sphingolipid profile in the CNS of the twitcher (globoid cell leukodystrophy) mouse: a lipidomics approach. *Cell. Mol. Biol.* **49:** 779–787.
13. Suzuki, K., Y. Suzuki, and K. Suzuki. 1995. Galactosylceramide lipidosis: globoid-cell leukodystrophy (Krabbe disease). *In* The Metabolic and Molecular Bases of Inherited Diseases. C. R. Scriver, A. L. Beaudet, W. S. Sly, and D. Valle, editors. McGraw-Hill, New York. 2671–2692.
14. Beutler, E., and G. A. Grabowski. 1995. Gaucher disease. *In* The Metabolic and Molecular Bases of Inherited Disease. C. R. Scriber, A. L. Beaudet, W. S. Sly, and D. Valle, editors. McGraw-Hill, New York. 2641–2670.
15. Kaye, E. M., and M. D. Ullman. 1984. Separation and quantitation of perbenzoylated glucocerebroside and galactocerebroside by high-performance liquid chromatography. *Anal. Biochem.* **138:** 380–385.
16. Parvathy, M. R., Y. Ben-Yoseph, D. A. Mitchell, and H. L. Nadler. 1987. Detection of Krabbe disease using tritiated galactosylceramides with medium-chain fatty acids. *J. Lab. Clin. Med.* **110:** 740–746.
17. Bosio, A., E. Binczek, W. F. Haupt, and W. Stoffel. 1998. Composition and biophysical properties of myelin lipid define the neurological defects in galactocerebroside- and sulfatide-deficient mice. *J. Neurochem.* **70:** 308–315.
18. Bichenkov, E., and J. S. Ellingson. 1999. Temporal and quantitative expression of the myelin-associated lipids, ethanolamine plasmalogen, galactocerebroside, and sulfatide, in the differentiating CG-4 glial cell line. *Neurochem. Res.* **24:** 1549–1556.
19. Kadowaki, H., K. E. Rys-Sikora, and R. S. Koff. 1989. Separation of derivatized glycosphingolipids into individual molecular species by high performance liquid chromatography. *J. Lipid Res.* **30:** 616–627.
20. Kushi, Y., C. Rokukawa, Y. Numajir, Y. Kato, and S. Handa. 1989. Analysis of underivatized glycosphingolipids by high-performance liquid chromatography/atmospheric pressure ionization mass spectrometry. *Anal. Biochem.* **182:** 405–410.
21. Costello, C. E., and J. E. Vath. 1990. Tandem mass spectrometry of glycolipids. *Methods Enzymol.* **193:** 738–768.
22. Kasama, T., and S. Handa. 1991. Structural studies of gangliosides by fast atom bombardment ionization, low-energy collision-activated dissociation, and tandem mass spectrometry. *Biochemistry.* **30:** 5621–5624.
23. Harvey, D. J. 1995. Matrix-assisted laser desorption/ionization mass spectrometry of sphingo- and glycosphingo-lipids. *J. Mass Spectrom.* **30:** 1311–1324.
24. Ii, T., Y. Ohashi, and Y. Nagai. 1995. Structural elucidation of underivatized gangliosides by electrospray-ionization tandem mass spectrometry (ESIMS/MS). *Carbohydr. Res.* **273:** 27–40.
25. Gu, M., J. L. Kerwin, J. D. Watts, and R. Aebersold. 1997. Ceramide profiling of complex lipid mixtures by electrospray ionization mass spectrometry. *Anal. Biochem.* **244:** 347–356.
26. Olling, A., M. E. Breimer, E. Peltomaa, B. E. Samuelsson, and S. Ghardashkhani. 1998. Electrospray ionization and collision-induced dissociation time-of-flight mass spectrometry of neutral glycosphingolipids. *Rapid Commun. Mass Spectrom.* **12:** 637–645.
27. Guittard, J., X. L. Hronowski, and C. E. Costello. 1999. Direct matrix-assisted laser desorption/ionization mass spectrometric analysis of glycosphingolipids on thin layer chromatographic plates and transfer membranes. *Rapid Commun. Mass Spectrom.* **13:** 1838–1849.
28. Levery, S. B., M. S. Toledo, R. L. Doong, A. H. Straus, and H. K. Takahashi. 2000. Comparative analysis of ceramide structural modification found in fungal cerebrosides by electrospray tandem mass spectrometry with low energy collision-induced dissociation of Li^+ adduct ions. *Rapid Commun. Mass Spectrom.* **14:** 551–563.
29. Sullards, M. C., D. V. Lynch, A. H. Merrill, Jr., and J. Adams. 2000. Structure determination of soybean and wheat glucosylceramides by tandem mass spectrometry. *J. Mass Spectrom.* **35:** 347–353.
30. Hsu, F. F., and J. Turk. 2001. Structural determination of glycosphingolipids as lithiated adducts by electrospray ionization mass spectrometry using low-energy collisional-activated dissociation on a triple stage quadrupole instrument. *J. Am. Soc. Mass Spectrom.* **12:** 61–79.
31. Han, X., and R. W. Gross. 2003. Global analyses of cellular lipidomes directly from crude extracts of biological samples by ESI mass spectrometry: a bridge to lipidomics. *J. Lipid Res.* **44:** 1071–1079.

32. Han, X., and R. W. Gross. 2004. Shotgun lipidomics: electrospray ionization mass spectrometric analysis and quantitation of the cellular lipidomes directly from crude extracts of biological samples. *Mass Spectrom. Rev.* First published on June 18, 2004; doi:10.1002/mas.20023. In press.
33. Griffiths, W. J. 2003. Tandem mass spectrometry in the study of fatty acids, bile acids, and steroids. *Mass Spectrom. Rev.* **22:** 81–152.
34. Pulfer, M., and R. C. Murphy. 2003. Electrospray mass spectrometry of phospholipids. *Mass Spectrom. Rev.* **22:** 332–364.
35. Welti, R., and X. Wang. 2004. Lipid species profiling: a high-throughput approach to identify lipid compositional changes and determine the function of genes involved in lipid metabolism and signaling. *Curr. Opin. Plant Biol.* **7:** 337–344.
36. Han, X., J. Yang, H. Cheng, H. Ye, and R. W. Gross. 2004. Towards fingerprinting cellular lipidomes directly from biological samples by two-dimensional electrospray ionization mass spectrometry. *Anal. Biochem.* **330:** 317–331.
37. Bligh, E. G., and W. J. Dyer. 1959. A rapid method of total lipid extraction and purification. *Can. J. Biochem. Physiol.* **37:** 911–917.
38. Folch, J., M. Lees, and G. H. Sloane Stanley. 1957. A simple method for the isolation and purification of total lipids from animal tissues. *J. Biol. Chem.* **226:** 497–509.
39. Han, X., and R. W. Gross. 1995. Structural determination of picomole amounts of phospholipids via electrospray ionization tandem mass spectrometry. *J. Am. Soc. Mass Spectrom.* **6:** 1202–1210.
40. Han, X., and R. W. Gross. 2001. Quantitative analysis and molecular species fingerprinting of triacylglyceride molecular species directly from lipid extracts of biological samples by electrospray ionization tandem mass spectrometry. *Anal. Biochem.* **295:** 88–100.
41. Han, X. 2002. Characterization and direct quantitation of ceramide molecular species from lipid extracts of biological samples by electrospray ionization tandem mass spectrometry. *Anal. Biochem.* **302:** 199–212.
42. Zhu, J., and R. B. Cole. 2000. Formation and decomposition of chloride adduct ions. *J. Am. Soc. Mass Spectrom.* **11:** 932–941.
43. Brugger, B., G. Erben, R. Sandhoff, F. T. Wieland, and W. D. Lehmann. 1997. Quantitative analysis of biological membrane lipids at the low picomole level by nano-electrospray ionization tandem mass spectrometry. *Proc. Natl. Acad. Sci. USA.* **94:** 2339–2344.
44. Blom, T. S., M. Koivusalo, E. Kuismanen, R. Kostiainen, P. Somerharju, and E. Ikonen. 2001. Mass spectrometric analysis reveals an increase in plasma membrane polyunsaturated phospholipid species upon cellular cholesterol loading. *Biochemistry.* **40:** 14635–14644.
45. Welti, R., W. Li, M. Li, Y. Sang, H. Biesiada, H-E. Zhou, C. B. Rajashekar, T. D. Williams, and X. Wang. 2002. Profiling membrane lipids in plant stress responses. Role of phospholipase Dα in freezing-induced lipid changes in Arabidopsis. *J. Biol. Chem.* **277:** 31994–32002.
46. Ekroos, K., I. V. Chernushevich, K. Simons, and A. Shevchenko. 2002. Quantitative profiling of phospholipids by multiple precursor ion scanning on a hybrid quadrupole time-of-flight mass spectrometer. *Anal. Chem.* **74:** 941–949.
47. Vos, J. P., M. Lopes-Cardozo, and B. M. Gadella. 1994. Metabolic and functional aspects of sulfogalactolipids. *Biochim. Biophys. Acta.* **1211:** 125–149.